J Appl Electrochem (2009) 39:1911–1916
DOI 10.1007/s10800-009-9899-x

ORIGINAL PAPER

Structure, microstructure and corrosion properties of brush-plated Cu–Ni alloy

N. Rajasekaran · S. Mohan

Received: 26 November 2008 / Accepted: 14 April 2009 / Published online: 30 April 2009

Abstract Cu–Ni alloy coatings on copper substrate by the brush-plating process have been investigated using XRD and AFM. The X-Ray diffraction analysis revealed that the brush-plated Cu–Ni alloy was heterogeneous and composed of cubic $Cu_{3.8}Ni$ phases. Uniform surface coverage of the substrate by granular morphology was observed from AFM. The corrosion protection performance of the brush-plated Cu–Ni alloy on copper substrate has been assessed using electrochemical corrosion tests. These results indicated a high charge transfer and low I_{corr} for the alloy system compared with copper deposits and the copper substrate.

Keywords Brush plating · XRD · Cu–Ni alloy · Corrosion resistance

1 Introduction

Cu–Ni alloy have superior anti-corrosion and strength properties [1]. Cu–Ni alloys are commonly used in various sea water applications such as valves, fittings condenser, and heat exchanger tubes. In addition to their good machinability, they posses excellent thermal and electrical properties and particularly resistance to biofouling. These Cu–Ni alloys with various compositions are difficult to obtain by electrodeposition, since the standard electrode potentials of Cu and Ni differ by approximately 600 mV. A complexing agent is required for the deposition of Cu–Ni alloy: cyanide [2], pyrophosphate [3], glycine [1], and citrate [4–6] were used as a complexing agent. In this perspective, this study aims to study the formation of Cu–Ni alloy from the sulphate/citrate electrolyte by brush-plating technique and to evaluate their characteristic properties. The tri-sodium citrate was chosen as the complexing agent due to its ability to improve the deposition efficiency, ability to obtain stress-free deposits. and its relatively less toxic nature.

The brush-plating technique, different from conventional plating, is an electrochemical process conducted with an electrolyte applied to the substrate by brush to form the adherent deposit [7–9]. Most metals used in conventional electrodeposition can be brush plated; the main applications are for repair and resizing purposes. Due to its portability, flexibility, and operational ease, brush plating has found increasing use in industry. Dini [10] summarized quantitative property data on a variety of brush-plated deposits, which offer promise in applications involving wear and corrosion resistance. A schematic of the brush-plating process is shown in Fig. 1

2 Experimental procedure

The Cu–Ni alloy coatings were brush plated on copper substrate. In this study, commercially available brush-plating equipment, Selectron power pack, USA, Modal 20 A - 60 V was utilized. The bath composition and bath parameter used for the Cu–Ni alloy depositions are shown in Table 1. Solutions were prepared from reagent grade chemicals and distilled water. Copper substrate were polished mechanically and degreased with acetone. After electrochemical cleaning with alkali solution and rinsing with distilled water the specimens were used for brush plating. The structural characterization of the deposits was carried out by XRD using Philips Diffractometer. The

N. Rajasekaran · S. Mohan (✉)
Central Electrochemical Research Institute, Karaikudi 630 006, India
e-mail: sanjnamohan@yahoo.com

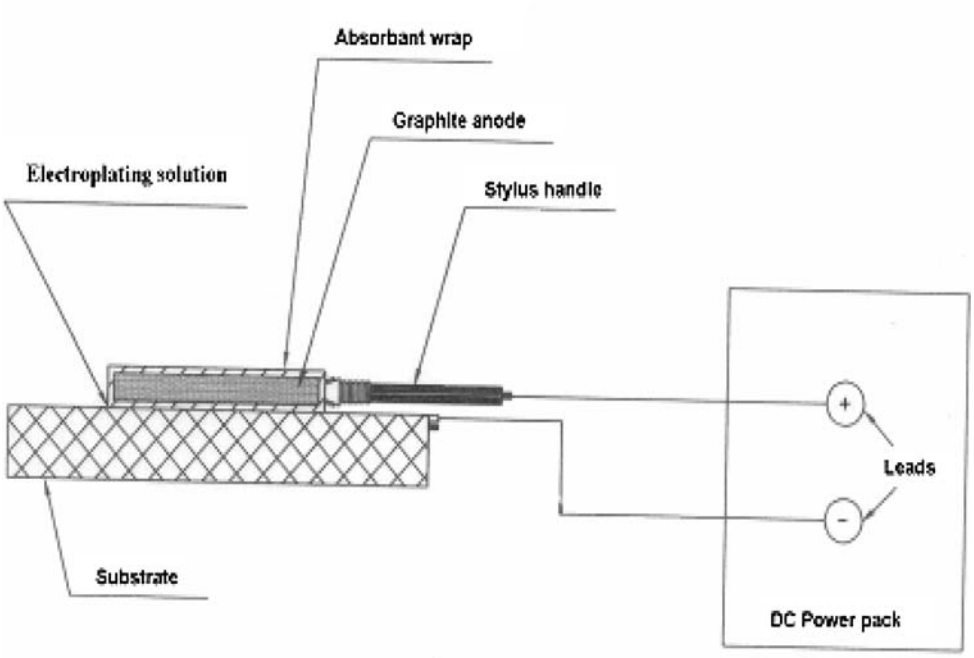

Fig. 1 Schematic of brush-plating process

Table 1 Bath composition and parameter for the brush-plated Cu–Ni alloy film

$CuSO_4$	0.02 M
$NiSO_4$	0.15 M
Tri-Sodium citrate	0.1 M
pH	4
Bath temperature	Room temperature
Plating voltage	4 V
Anode	Graphite stylus

surface morphology examinations were carried out by Molecular imaging Atomic force microscope (AFM). The micro hardness of the brush-plated sample was determined using Everone micro hardness testing machine with a Vickers indenter (load 25 g). The corrosion resistance of the deposit was assessed by electrochemical polarization studies and impedance measurement using Parstat 2273 Advanced electrochemical analyzer. Experiments were carried out using the standard three-electrode configuration, saturated calomel as a reference electrode, platinum foil as a counter electrode and the sample as the working electrode. Specimens of size 1 cm^2 were immersed in the test solution of 3.5 wt% NaCl at room temperature for corrosion studies

3 Result and discussion

The Cu–Ni alloy brush plated from the sulphate/citrate bath under optimized condition was adherent, smooth, and bright in appearance. The brush-plated Cu–Ni alloy samples were bent through an angle of 180° repeatedly and incurred no lifting and peeling off which showed good adhesion of these coatings to the copper substrate. Deposits with Vickers hardness of 376 Hv (25 g) were obtained for the optimized Cu–Ni alloy samples. This is average value taken after indentation at five different places of deposits. This higher value of hardness in the brush-plated alloy is due to the smaller grain size in the order of nanometer [11]. The effect of plating time on the plating thickness is shown in Fig. 2. It is seen that the coating thickness increases with increasing plating duration.

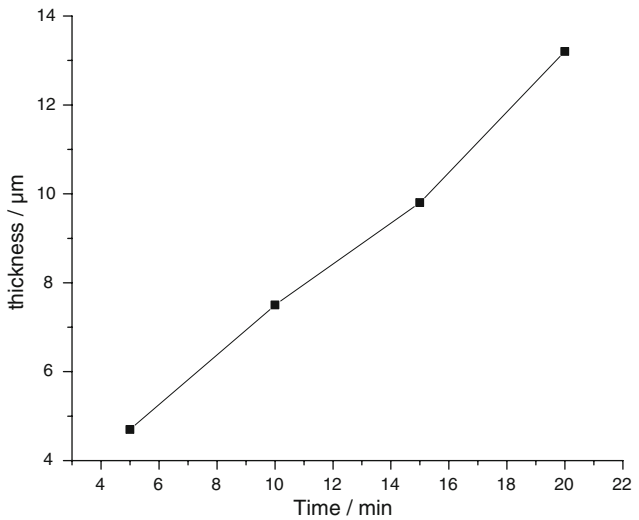

Fig. 2 Plating thickness as a function of plating time

3.1 Structure of the deposits

The X-ray diffractogram (XRD) obtained for the brush-plated Cu–Ni alloy from the sulphate/citrate bath is shown in Fig. 3. The observed crystallographic distance, d (h k l), and expected values from phases described in JCPDS are shown in Table 2. The data show that the observed d values are in good agreement with the standard d values reported in JCPDS of the corresponding phases. The phases, $Cu_{3.8}Ni$ and Ni, are observed in the face centered cubic structure. The crystalline size (D) was calculated from the line broadening, β, under simple assumption that the line broadening is caused by the crystalline size alone [12].

$$D = \frac{0.9\lambda}{\beta\cos\theta}$$

where λ is the X-Ray wavelength and θ is Bragg angle. The crystalline sizes were calculated for different phases present in the film and are given in Table 3. The crystalline sizes were found to be in the range of 20–50 nm. Such small crystalline sizes not only contribute to the smooth surface morphology but also have a beneficial effect on the improvement of microhardness of the coatings [11]. Furthermore, the crystalline size reduction to the nanometer range results in considerable improvement in their corrosion resistance [13].

The strain and the dislocation density are also determined from the XRD data using the equation [14]

$$\varepsilon = \frac{\beta\cos\theta}{4} \text{ and } \delta = \frac{n}{D^2}$$

Table 2 Comparison of standard interplanar distance with observed interplaner distance of the XRD pattern of brush-plated Cu–Ni alloy film

2θ	d-observed	d-standard	hkl	Relative intensity (%)	Phase
43.3464	2.085	2.080	111	100.0	$Cu_{3.8}Ni$
44.4377	2.037	2.034	111	18.60	Ni
50.4860	1.806	1.797	200	33.97	$Cu_{3.8}Ni$
51.7928	1.763	1.762	200	2.250	Ni
74.0742	1.278	1.269	220	5.730	$Cu_{3.8}Ni$
89.7764	1.091	1.084	311	11.40	$Cu_{3.8}Ni$
94.9415	1.045	1.037	222	7.590	$Cu_{3.8}Ni$

Table 3 Crystalline size and lattice parameter of the Cu–Ni alloy film

Phase	JCPDS card	Lattice parameter a (Å)	Crystalline size (nm)
$Cu_{3.8}Ni$	9-0205	3.595	50.7
Ni	4-0850	3.523	15.0

where β is the FWHM of (111) peak, D is crystalline size, and n is a factor, which is unity for thin film [15]. The calculated value of the strain and the dislocation densities are 3.7×10^{-2}, 3.8×10^{-4}. The smaller values of strain and dislocation density indicate the high quality deposits.

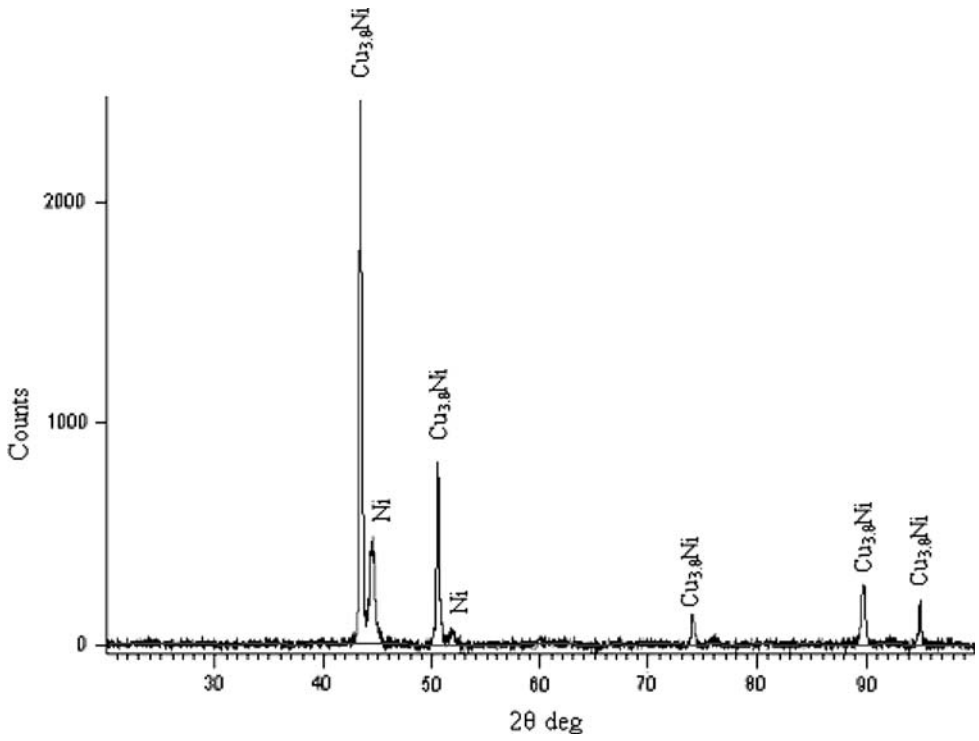

Fig. 3 X-ray diffragrom of the brush-plated Cu–Ni alloy film

3.2 Potentiodynamic polarization

The potentiodynamic polarization curves obtained for the Cu substrate, brush-plated Cu, and Cu–Ni alloy on Cu substrate sample in 3.5 wt % NaCl electrolyte are presented in Fig. 4. The E_{corr} and I_{corr} values were calculated using the Tafel extrapolation method and values are given in Table 4. There is an appreciable increase in corrosion resistance for the Cu–Ni alloy on Cu substrate compared to that for Cu deposits and Cu substrate, which is due to passive film on the surface [16]. E_{corr} and I_{corr} values improve (a less negative value of E_{corr} and lower value of I_{corr} signifies an improvement in corrosion resistance) for the Cu–Ni alloy on Cu substrate. The porosity of the coatings is determined using the formula

$$P = \frac{R_{P,S}}{R_p} 10^{-|\Delta E\text{corr}|/\text{ba}}$$

where

$R_{P,S}$ - substrate polarization resistance
R_P - coatings polarization resistance

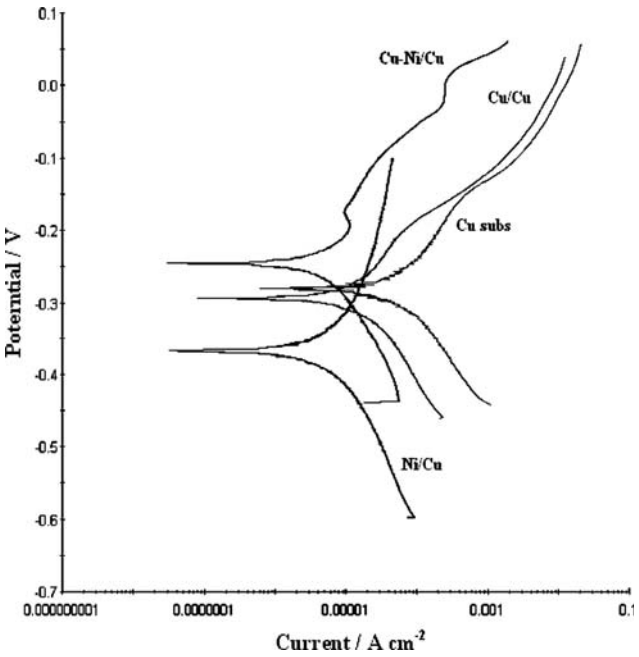

Fig. 4 Comparative potentiodynamic polarization curve of Cu–Ni alloy, Cu/Cu, and Cu substrate

ΔE_{corr} - potential difference between the coatings and substrate
ba - anodic slope for substrate

The porosities of Cu–Ni alloy, Cu coated and the copper substrates are determined using the above formula and tabulated in Table 4. The porosity of the Cu–Ni alloy coatings are low compared to that of Cu deposits. So the Cu–Ni alloys have better corrosion resistance than Cu deposits and copper substrate.

3.3 Electrochemical impedance

The electrochemical impedance spectra of brush-plated Cu–Ni alloy systems were measured with the same three-electrode system as was used for the potentiodynamic polarization experiments. Impedance measurements were made at 10 mV in the frequency range of 10–100 Hz. The impedance results obtained from Nyquist plots for the sample used for the corrosion tests in 3.5 wt% NaCl solutions are shown in Table 5 and Fig. 5. The charge transfer resistance R_{ct} can be related to I_{corr} [17]

$$R_{ct} = \frac{\text{ba} \times \text{bc}}{2.3\,(\text{ba} + \text{bc})} \times I_{corr}$$

where R_{ct} is charge transfer resistance, and ba and bc are the anodic and cathodic slopes.

The double layer capacitance C_{dl} value is obtained from the frequency at which Z imaginary is maximum [15]

$$\Omega\left(Z_{(im)}\,\text{max}\right) = \frac{1}{C_{dl}R_{ct}}$$

The increased R_{ct} values and decreased C_{dl} values for the Cu–Ni alloy clearly confirm the better corrosion resistance of these systems compared to Cu deposits and Cu substrate. Furthermore, more pronounced semicircular region is

Table 5 Corrosion parameter obtained from the impedance measurement by Nyquist plots

Sample	OCP (V)	R_{ct} (Ω cm^{-2})	C_{dl} (μF cm^{-2})
Cu–Ni/Cu	−0.221	3933	216
Cu/Cu	−0.204	1105	1798
Cu subs	−0.183	952	353

Table 4 Corrosion parameter obtained from the polarization studies in 3.5 wt % NaCl

Sample	E_{corr} Vs SCE (mV)	ba (mV dec^{-1})	bc (mV dec^{-1})	I_{corr} (μA cm^{-2})	Corrosion rate (mpy)	Porosity (%)
Cu–Ni/Cu	−245.2	140.1	145.9	3.925	1.703	0.167
Cu/Cu	−293.6	103.8	125.9	12.55	5.751	0.196
Cu subs	−279.5	121.7	132.6	54.5	24.91	–

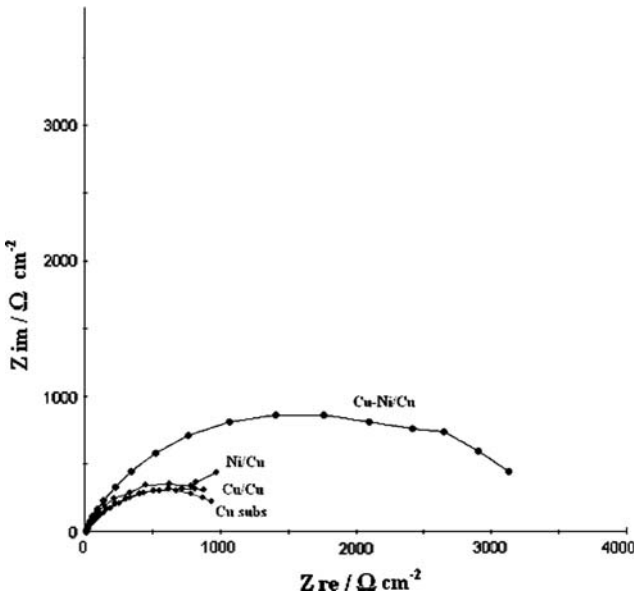

Fig. 5 Nyquist plots for corrosion measurement of Cu–Ni alloy, Cu/Cu, and Cu substrate

observed in the case of Cu–Ni alloy sample indicating that the system has a good corrosion resistance.

3.4 Surface morphology

Surface morphology and topography of the brush-plated Cu–Ni alloy samples were carried out using atomic force microscopy (AFM). The advantage of AFM is its capacity to probe minute details related to the individual grains and intergrain region. A representative AFM picture, scanned over an area of 5 × 5 μm of the Cu–Ni alloy sample prepared under optimized conditions, is shown in Fig. 6a, b. This image shows that the deposits have finer nodular grains in the range of 100–400 nm showing uniform coverage. Actually, the grains and crystals are totally different. The grains are made up of few crystals: crystalline sizes are calculated from XRD technique using Scherrer's formula, grains sizes are calculated from the AFM technique; hence, the size differences occurring between the grain and crystalline size as well as the cross sectional AFM images are included in the figure which shows smaller grains.

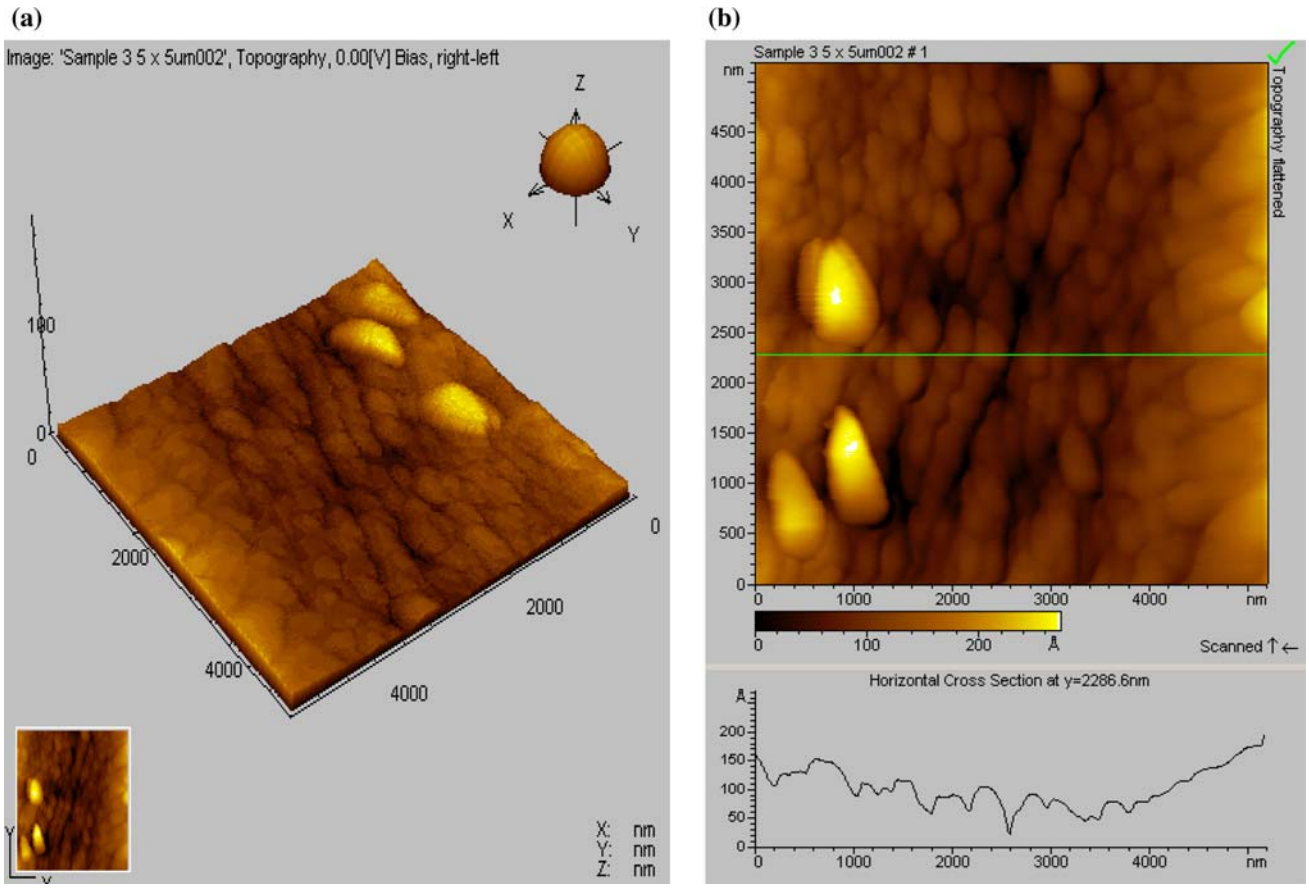

Fig. 6 Atomic force microscopy of the brush-plated Cu–Ni alloy film

Roughness analysis of these coatings was carried out and the average roughness (*Ra*) value was calculated as the deviation in hight from the profile mean value [18]

$$Ra = 1/N \sum_{0}^{N} |Z_i - Z|$$

where

Z_i - the hight of the each pixel position along the line profile
Z - The mean hight
N - Number of pixels along the each line scan of the profile

The roughness value of the alloy deposition is 0.35 μm. This value indicates that the depositions are smoother

4 Conclusion

Adherent, smooth, and bright deposits of Cu–Ni alloy were brush plated successfully on copper substrates from Sulphate/citrate baths. The brush-plated Cu–Ni alloy films are heterogeneous systems. Corrosion measurement shows the appreciable increase in corrosion resistance for the brush-plated Cu–Ni alloy on the copper substrate. Uniform coverage with the spherical nodular morphology of these coatings is observed from microstructure analysis. The Cu–Ni alloy coatings obtained from the bath composition and bath parameters mentioned demonstrate excellent corrosion protective performance.

References

1. Mizushima I, Chikazawa M, Watanabe T (1996) J Elecrochem Soc 143:1978
2. Stout LE, Burch OG, Langdorf AS (1930) Trans Elecrochem Soc 57:113
3. Ishikawa M, Enomoto H (1980) J Met Finish Soc Jpn 31:545
4. Meuleman WRA, Roy S, Peter L, Bakonyi I (2004) J Electrochem Soc 151(4):C256
5. Bakonyi I, Toth J, Kiss LF, Toth-kadar E, Peter L, Dinia A (2004) J Magn Magn Mater 269:156
6. Baskaran I, Shankaranarayanan TSN, Stephen A (2006) Meter Lett 60:1990
7. Du L, Xu B, Dong S, Yang H, Wu Y (2005) Surf Coat Technol 192:311
8. Subramanian B, Mohan S, Shoba Jayakrishnan, Jayachandran M (2007) Curr Appl Phys 7:305
9. Subramanian B, Mohan S, Shoba Jayakrishnan, Jayachandran M (2006) Surf Coat Technol 201:1145
10. Dini JW (1997) Met Finish 95(6):88
11. Kim SH, Erb U, Aust KT, Ganzalaz F, Palumbo G (2004) Plat Surf Finish 5:68
12. Koch M, Ebarbach U (1997) Surf Eng 13(2):157
13. Mu Haichuan, Seok Jin, Lin RY (2003) J Electrochem Soc 150(2):C67
14. Williamson GB, Smallman RC (1956) Philos Mag 1:34
15. Senthilkumar V, Venkatachalam S, Viswanathan C, Gopal S, Narayanadass Sa K, Mangalaraj D, Wilson KC, Vijayakumar KP (2005) Cryst Res Tech 40:573
16. Rafaey SAM, Taha F, Hasanin THA (2004) Appl Surf Sci 227:416
17. Subramanian B, Mohan S, Shoba Jayakrishnan, Jayachandran M (2007) J Appl Electrochem 37:219
18. Smith James R, Breakspear S, Cambell SA (2003) Trans Inst Met Fin 81:B55